Dissociation and Multiply Charged Silicon Ejection in High Abundance from Hexamethyldisilane

ARTICLE *in* THE JOURNAL OF PHYSICAL CHEMISTRY A · OCTOBER 2010

Impact Factor: 2.69 · DOI: 10.1021/jp1067186 · Source: PubMed

2 AUTHORS:

Tomoyuki Yatsuhashi
Osaka City University
64 PUBLICATIONS **908** CITATIONS
SEE PROFILE

Nobuaki Nakashima
Toyota Physical and Chemical Institute
214 PUBLICATIONS **4,165** CITATIONS
SEE PROFILE

Dissociation and Multiply Charged Silicon Ejection in High Abundance from Hexamethyldisilane

Tomoyuki Yatsuhashi*,†,‡ and Nobuaki Nakashima†

Department of Chemistry, Graduate School of Science, Osaka City University, 3-3-138 Sugimoto, Sumiyoshi, Osaka 558-8585 Japan, and PRESTO, Japan Science and Technology Agency (JST), 4-1-8 Honcho Kawaguchi, Saitama, 332-0012 Japan

Received: July 19, 2010; Revised Manuscript Received: October 5, 2010

Quadruply charged, neon-like silicon and helium-like carbon were generated by the exposure of hexamethyldisilane to intense femtosecond laser pulses. Dissociation of the silicon−silicon bond, the formation of highly charged silicons, as well as the saturation intensity of their formation were studied by mass spectroscopy. The production of these ions in high abundance, but also with lower laser intensity than theoretically expected for the element, was accomplished by using organosilicon compounds. Multiply charged silicon was generated at low laser intensity because stripping electrons from organosilicon compounds is much easier than from pure silicon due to the loose binding of electrons belonging to molecular orbitals. Femtosecond laser ionization is a valuable methodology for producing highly charged ions in high abundance and is useful in many fields of interest.

Introduction

Silicon carbide thin film has attracted much attention in relation to power devices, light-emitting diodes, diode lasers, magnetic disks, and also hard coatings.[1] These films have been prepared by thermal chemical vapor deposition (CVD) and plasma CVD[2] using the electron and/or ion beam evaporation methods.[3] Silanes are important chemical reactants in the preparation of such films. As a result of decomposition during evaporation processes, fragment ions such as Si, C, C_nH_m, and SiC_nH_m are deposited on the substrate. Such ions can be generated by conventional ion sources, such as a Freeman-type ion source;[4] however, multiply charged silicon has not yet been utilized for the deposition process due to the lack of an efficient production methodology. Although they are not conventional, electron cyclotron resonance and electron ion beam trap methods are powerful generators of highly charged ions.[5] Intense femtosecond laser ionization is a promising methodology to produce highly charged ions by stripping many electrons spontaneously by nonresonant multiphoton and/or tunnel ionization processes.[6] High energetic multiply charged atomic ions were obtained as a result of Coulomb explosion of highly charged molecule. We can produce intact molecular ions,[7] multiply charged molecular ions,[8] and also highly charged atomic ions[9] in the gas phase by optimizing laser parameters at ambient temperature. In contrast, singly charged fused ions can be produced in the solid phase due to high density.[10] Intact molecular ion formation is one of the distinguishing features of using femtosecond laser pulses for analytical purposes.[11] To achieve intact ion formation, not only pulse width[12] and polarization[13] but also laser wavelength[14] should be optimized. As for the molecular ions, C_{60}^{12+} is the highest charged state ever observed,[15] and a quadruply charged state is the maximum charge state in the case of common hydrocarbons.[16] The formation of a variety of multiply charged atomic ions has also been reported. These include both metal ions[17] and nonmetal ions, especially halogens[18] and rare gases.[9] However, the formation of highly charged silicon has only been reported by Castillejo et al. at laser intensities up to 2×10^{14} W cm^{-2}.[19,20]

After the efficient production of a highly charged atomic ion with high kinetic energy by exposure to intense femtosecond laser pulses, it may be worth trying to select specific ions such as H^+, C^{x+}, $C_nH_m^+$, Si^{y+}, and $SiC_nH_m^+$ with a mass spectrometer equipped with an ion deflector (mass gate), and thus control the composition ratio of the deposited films. The state-of-the-art technology enables us to produce multi-mJ and multi-kHz repetition rate laser pulses, which would be sufficient to achieve efficient ion production. The deposition of highly charged energetic ions should affect the properties of the deposited films due to their high electron affinity. In the present study, we generated an abundance of highly charged silicon from hexamethyldisilane under intense femtosecond laser fields. The dissociation process and also ion distribution was studied by mass spectroscopy. We focused our attention on the dissociation of the silicon−silicon bond, the formation of highly charge silicon ions, as well as the saturation intensity of their formation. The main dissociation channel is the Si−Si bond cleavage forming trimethylsilyl cations, but Coulomb explosions forming trimethylsilyl cations also occurred. Quadruply charged, neon-like silicon and helium-like carbon was the highest charge state observed. Highly charged silicon was obtained in abundance at a lower laser intensity than that theoretically expected for the element.

Experimental Section

Hexamethyldisilane (HMDS, $C_6H_{18}Si_2$, Aldrich) and xenon (Japan Air Gases, 99.99%) were introduced by a leak valve. The chamber pressure was monitored 20 cm away from the laser focus point with a cold cathode pressure gauge. The base pressure of the ionization chamber and the time-of-flight chamber was below 5×10^{-7} Pa. The sample pressure in the ionization chamber was kept below 5×10^{-5} Pa during the

* To whom correspondence should be addressed. Phone: +81-6-6605-2554. Fax: +81-6-6605-2522. E-mail: tomo@sci.osaka-cu.ac.jp.
† Osaka City University.
‡ Japan Science and Technology Agency.

10.1021/jp1067186
Published on Web 10/19/2010

experiments to avoid the space-charge effect. The pressure of the time-of-flight mass chamber was 10 times below the ionization chamber by differential pumping to avoid collision-induced fragmentation. A 0.5 TW all-diode pumped Ti:Sapphire laser (Thales Laser, Alpha 100/XS, < 30 fs, 100 Hz, > 15 mJ, 800 nm, rms stability 1%) was used in this study. The pulse width was measured by a second-order single-shot autocorrelator (Thales Laser, TAIGA). The laser beam passes through several materials, such as a beam splitter (quartz, $t = 1$ mm), a focusing lens (quartz, $t = 5$ mm), and an ionization chamber window (quartz, $t = 3$ mm). The same materials were placed in front of the autocorrelator, and group velocity dispersions introduced by these materials were compensated with the acoustoptic programmable dispersive filters (Fastlite, Dazzler) to have the minimum pulse width. We did not achieve gain narrowing compensation by Dazzler, and the typical pulse width was 45 fs.

A linear mode of reflectron-type time-of-flight mass spectrometer (TOYAMA, KNTOF-1800) was used for ion analysis. The acceleration voltage was 4000 V, and the extraction field potential (303 V cm^{-1}) was optimized to have the similar height of double peaks originated in Coulomb explosion. In the intensity dependence experiments, the extraction field potential (833 V cm^{-1}) was applied to have better mass resolution and higher signal intensity. The resolution ($m/\Delta m$, fwhm) was 560 (303 V cm^{-1}) and 1000 (833 V cm^{-1}) at $m/z = 129$. The output signal from a MCP (Hamamatsu, F4655−11X) was averaged by a digital oscilloscope (LeCroy, Wave Runner 6100, 1 GHz) for 1000 shots. The ion yield was obtained by integrating over the appropriate peaks in the time-of-flight spectrum. A slit of 500 μm width was located on the extraction plate perpendicular to the laser propagation direction in order to collect the ion that was generated in the most tightly focused point of the laser beam (achieving ion collection from axially symmetric parallel beam geometry). The direction of the laser polarization (800 nm, linear) against the time-of-flight axis was changed by a zero-order half-wave plate and was confirmed using a broadband polarizing cube beam splitter. The laser beam was focused into the ionization chamber with a planoconvex quartz lens of 200 mm focusing length. The position of the lens was adjusted to have a maximum signal intensity of the highest charge state of xenon observed (Xe^{4+} or Xe^{5+}). The laser energy was attenuated by the combination of a half-wave plate and plate polarizers. A part of the laser beam was reflected by a beam splitter at a small incident angle, and the laser pulse energy was measured using an integrating sphere (Labsphere, Spectralon coating) and a calibrated Si pin-photodiode. The actual laser intensity of the linear polarized pulse at the focus was determined by measuring the saturation intensity, I_{sat} of xenon (1.1×10^{14} W cm^{-2} for a 45 fs pulse) by the method of Hankin et al.[21] The ions of the HMDS were measured successively after the measurement of I_{sat} of xenon without, between two runs, changing experimental conditions.

Results and Discussion

Dissociation of Hexamethyldisilane with Femtosecond Laser Pulses. Figure 1 shows the time-of-flight mass spectra of hexamethyldisilane (HMDS) at different laser intensities. At laser intensities around 10^{13} W cm^{-2}, the principal ions were the molecular ion (M^+) and trimethylsilyl cation ($M^+/2$, $(CH_3)_3Si^+$), which was produced by the dissociation of a central Si−Si bond. As clearly shown in Figure 1, the moderate dissociative ionization of HMDS was achieved by using femtosecond laser pulses. The ratio of M^+ ($m/z = 146$) to $M^+/2$

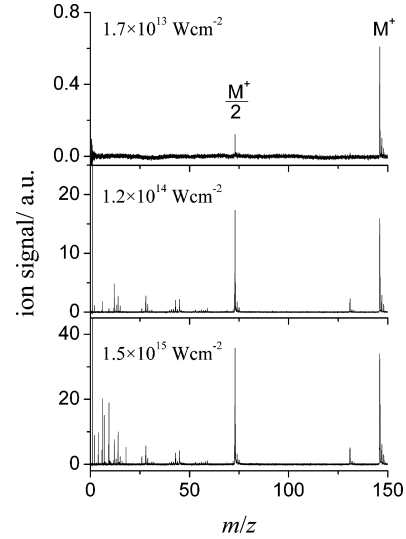

Figure 1. Time-of-flight mass spectra of HMDS at different laser intensities. The laser polarization is parallel to the ion flight axis. The extraction field potential is 833 V cm^{-1}. The peak of H^+ is out of range (middle and bottom panels).

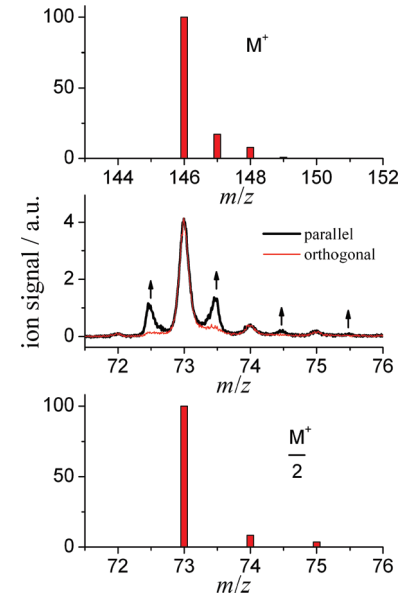

Figure 2. Mass spectra of HMDS. The upper panel is the expected isotope pattern of the molecular ion (M^+). The middle panel shows the experimental data at 3.3×10^{14} W cm^{-2}. The laser polarization is parallel (bold line) and orthogonal (thin line) to the ion flight axis. The extraction field potential is 303 V cm^{-1}. The bottom panel is the expected isotope pattern of $M^+/2$ (trimethylsilyl cation).

($m/z = 73$) was 5.9 at 1.7×10^{13} W cm^{-2} in this study, whereas it was 1.0 and 0.11 with 10 and 70 eV of electron impact, respectively.[22]

Figure 2 shows the magnified mass spectrum around $m/z = 73$. It should be identified first whether this peak is originated in doubly charged molecular ion or trimethylsilyl cation. The upper, middle, and lower panels of Figure 2 are an expected isotope pattern of the molecular ion, experimental data at 3.3×10^{14} W cm^{-2}, and an expected isotope pattern of $M^+/2$, respectively. The doubly charged molecular ion (M^{2+}) should have the same ion intensity distributions as a singly charged molecular ion. In addition, a doubly charged molecular ion would be definitively identified by isotope peaks of noninteger charge-to-mass ratio and a narrower peak width than that of singly charged ions. In this sense, a peak at $m/z = 73.5$ could

be the isotope peak of M^{2+}; however, the peak intensity strongly depended on the configuration between the direction of laser polarization and the ion flight axis. When the direction of laser polarization was parallel to the ion flight axis, this situation is referred to as the "parallel condition." If the laser polarization direction is orthogonal to the ion flight axis, it is the "orthogonal condition." The peak at $m/z = 73.5$ was suppressed under the orthogonal condition; however, the yield of molecular ion should be independent of the configuration due to its nearly zero kinetic energy, thus all of the molecular ions can path through a narrow slit located on the extraction plate. In contrast, the detection of fragment ions with certain kinetic energy was limited by the slit because the stripping of electrons from molecules has large probability along the molecular axis, and energetic ions were emitted along the laser polarization direction. As a result, the yield of energetic fragment ions ejected along laser polarization direction (molecular axis) was suppressed under orthogonal condition. When the precursor ion has longer lifetime than rotational time constant, fragment ions were emitted in an isotropic manner. Molecular frame distortion and/or ionization with a larger fraction of the randomly oriented molecules are considered to be the reason for the isotropic emission at higher laser intensity. On the basis of the peak intensity variations, the experimentally observed ions at around $m/z = 73$ are assigned not as a doubly charged molecular ion but as an symmetrically split trimethylsilyl cation ($M^+/2$). The $M^+/2$ peak without kinetic energy originated from the fragmentation of the singly charged molecular ion with some excess energy, as is typical in electron-impact spectra. The origin of the peak splitting appeared to be the Coulomb explosion (charge separation processes) of fragment ions: the ions' forward and backward emissions against the flight axis.[23] Therefore, $M^+/2$ with kinetic energy appears as double peaks centered at $m/z = 73$, 74, and 75, respectively. The split components at $m/z = 73.5$ and 74.5 are overlapped with other split peaks. Thus, the ion yield of trimethylsilyl ions between $m/z = 72.5$ (forward peak) and 73 (center peak) is compared as a function of laser intensity in Figure 3a. As the laser intensity increased, the ratio increased and became saturated at around 1×10^{14} W cm^{-2}. From the degree of peak splitting, we estimated the kinetic energy of fragment ions using eq 1, where E_k, q, e, m, V_1, V_2, d, t_1, and t_0 are kinetic energy, charge number, elemental charge, mass of ion, voltage applied to repeller electrode, voltage applied to accelerating electrode, distance between repeller and acceleration electrodes, flight time of the ion emitted forward to the detector, and calculated flight time of ion with zero kinetic energy, respectively.

$$E_k = \frac{(qe)^2}{2m}\frac{(V_1 - V_2)^2}{d^2}(t_1 - t_0)^2 \quad (1)$$

As shown in Figure 3b, the kinetic energy of $M^+/2$ has a peak at 1.5 eV. The spectral features and peak position are independent of the laser intensity. Supposing that HMDS was split into two equivalent $M^+/2$ at the equilibrium internuclear distance carrying the same kinetic energy, then the kinetic energy of each $M^+/2$ was calculated to be 3.1 eV by eq 2.

$$E_k = \frac{qq'e^2}{4\pi\varepsilon_0 r} \quad (2)$$

Here, E_k, q, q', e, ϵ_0, and r are kinetic energy, charge number of observed ion, charge number of counterion, elemental charge, the dielectric constant in a vacuum, and the distance between ions (equibrium nuclear distance of Si−Si bond in the neutral state, 2.35 Å), respectively. The small (half) value of the observed kinetic energy is understood as the result obtained by stretching (twice) the molecular bond before the Coulomb explosion, as has been observed for light diatomic molecules.[24] The doubly charged molecular ion of HMDS is missing in the mass spectra, presumably because it has repulsive potential and hence ultrashort lifetime. On the basis of the kinetic enegy consideration, the origin of the forward peak of $M^+/2$ was concluded to be the doubly charge state of HMDS. The increase and saturation of the ion yield ratio of trimethylsilyl ions of $m/z = 72.5$ (forward peak) to 73 (center peak) shown in Figure 3a may reflect the variations of the precursor doubly charged molecular ion yield. The saturation may indicate that the further ionization and decomposition became dominant at high intensity and that the $M^+/2$ formation occurs in the wing of the laser focus where laser intensity is low.

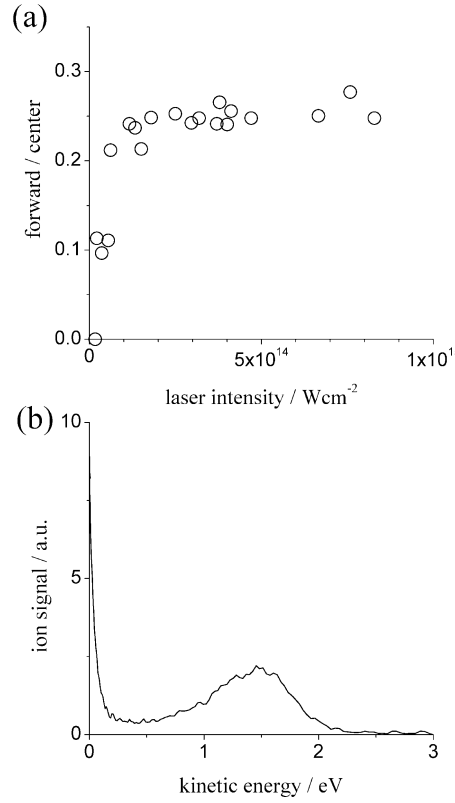

Figure 3. (a) The ratio of trimethylsilyl cation yield: ion centered at $m/z = 72.5$ (forward) to that at 73 (center). (b) The kinetic energy spectrum of trimethylsilyl cation. The laser polarization is parallel to the ion flight axis. The extraction field potential is 303 V cm^{-1}.

Ejection of Highly Charged Atomic Ions in High Abundance and at Low Laser Intensity. At higher laser intensity, violent fragmentation and highly charged atomic ion formation was observed. Many peaks originating in highly charged atomic ions became dominant in the mass spectra at $m/z < 15$ (Figure 1 bottom). These are H_n^+ ($n = 1-2$), C^{x+} ($x = 1-4$), and Si^{y+} ($y = 1-4$), respectively. The magnified spectrum is shown in Figure 4. The assignment of quadruply charged carbon was based on the peak position ($m/z = 3$) and the large extinction ratio between the orthogonal and parallel conditions. Quadruply charged states of silicon and carbon were the maximum charge states observed in this study. Their ionization potentials are 103 and 148 eV, respectively. It is therefore difficult to produce such ions from molecules, even with synchrotron radiation.[25] Qua-

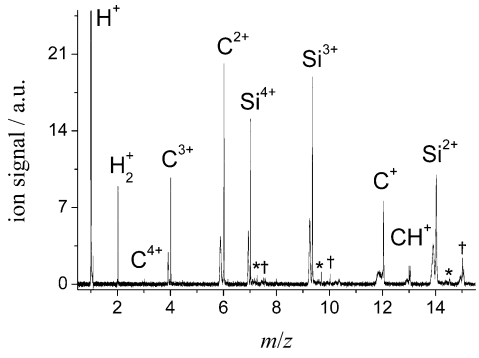

Figure 4. Time-of-flight mass spectra ($m/z < 15.5$) of HMDS at 1.5×10^{15} W cm^{-2}. The laser polarization is parallel to the ion flight axis. The asterisks and daggers indicate multiply charged SiH (*) and SiH_2 (†), respectively. The contribution of CH_3^+ could be predominant at $m/z = 15$. The peak of H^+ is out of range. The extraction field potential is 833 V cm^{-1}.

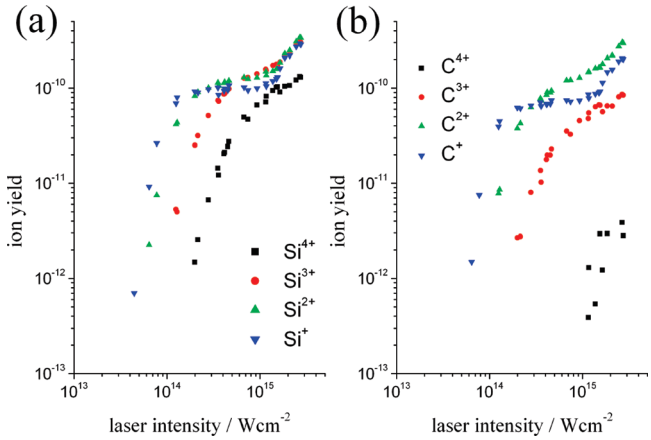

Figure 5. Ion yields of (a) silicon and (b) carbon as a function of laser intensity: singly charged ion (inverted triangle); doubly charged ion (triangle); triply charged ion (circle); and quadruply charged ion (square). The laser polarization is parallel to the ion flight axis.

druply charged silicon and carbon have the same electron configurations as neon (Si^{4+}) and helium (C^{4+}), meaning that their ionization energies are relatively large: 392 eV (C^{4+}); 167 eV (Si^{4+}). A much greater laser intensity would be required to create C^{5+} and Si^{5+}; however, C^{5+} has not been detected even at 10^{17} W cm^{-2}.[26] Figure 5 shows the ion yields as a function of laser intensity. As the laser intensity increased, the ion yield increased steeply until reaching the saturation region. After the saturation region, it again increased gently. All ions showed similar features, and this steplike behavior can be attributed to the volume effects.[27] The restriction of ion volume along the line of laser beam propagation (perpendicular to the ion extraction direction) was successfully achieved; however, restriction of the volume in the direction of ion extraction could not be achieved by placement of a slit. As the laser intensity increases, a higher charge state is formed at the most intense central part of the laser beam; in contrast, lower charged ions are produced at the wing of the laser beam. Thus, we compared an ion yield below the second increase. As was clearly observed, the relative ion yield among different charge states became closer as the laser intensity increased, and a large amount of quadruply charged silicon was obviously obtained. The relative abundances of multiply charged ions compared with singly charged ions are summarized in Table 1. The relative silicon ion yields from HMDS are also compared with those obtained from 2-chloro-ethenylsilane by 50 fs pulses.[19,20]

TABLE 1: Relative Abundance of Highly Charged Silicon[a]

	Si^+	Si^{2+}	Si^{3+}	Si^{4+}	laser intensity (10^{14} W cm^{-2})
HMDS	1	1.32	0.496	0.0797	3.3
HMDS	1	1.99	1.57	0.706	15
2-chloro-ethenylsilane[b]	1	0.28	9.5×10^{-2}	5.0×10^{-2}	1.9[c]

[a] Detector sensitivity was not corrected. [b] 1:3 mixture of cis and trans isomers. Ratio was calculated from the data in Figure 5 of ref 20. [c] 800 nm, 50 fs.

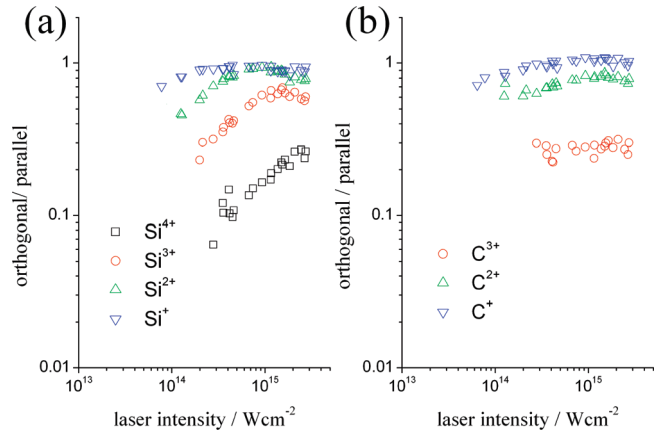

Figure 6. Ion yield ratios (orthogonal to parallel) of (a) silicon and (b) carbon as a function of laser intensity: singly charged ion (inverted triangle); doubly charged ion (triangle); triply charged ion (circle); and quadruply charged ion (square).

The peak and maximum kinetic energies of highly charged silicon at 1.5×10^{15} W cm^{-2} were: 6.8 and 30 eV (Si^{2+}); 17 and 45 eV (Si^{3+}); and 34 and 80 eV (Si^{4+}). The peak kinetic energies are defined as the mean energy in the whole spectral range at the signal measured under parallel condition. The maximum kinetic energies are defined as the energy where the ion intensity is 10% of the peak in the higher energy region of the signals measured under parallel condition. These peak values were two or three times smaller than those obtained from 2-chloro-ethenylsilane at 2×10^{14} W cm^{-2}: 26 eV (Si^{2+}); 55 eV (Si^{3+}); and 85 eV (Si^{4+}).[20] As kinetic energy depends on the charges and distance between ions as described by eq 2, the difference may come from the longer distance between charges by the elongation of the Si−Si bond before the Coulomb explosion in the case of HMDS and from the absence of chlorine, which can be charged up to four plus. Figure 6 compares the relative ion yield between the orthogonal and parallel conditions. As the laser intensity increased, the ion emissions became isotropic and the ratio reached nearly unity in the cases of Si^+, Si^{2+}, and C^+. This isotropic emission (broadening of the angular distribution) of ions at high laser intensity is presumably due to deformation of the molecular skeleton under strong laser electric fields and ionization with a larger fraction of the randomly oriented molecules.

There is no doubt that femtosecond laser ionization is a promising methodology to produce an abundance of highly charged ions; however, isolated molecules cannot acquire large kinetic energies because Coulomb repulsion within the framework of a molecule limits the maximum values. An extremely large (500 eV) kinetic energy release of Si^{4+} has been achieved from silicon clusters (nano particles) by femtosecond laser pulses at 10^{13} W cm^{-2};[28] however, a relative abundance of multiply charged silicon was not identified. The ease of ionization is another important issue when considering an ion source. We used the saturation intensity (I_{sat}) to quantitatively evaluate the

TABLE 2: Saturation Intensity (I_{sat}) of Highly Charged Silicon[a]

	I_{sat} (10^{14} W cm^{-2})			
ion source	Si^+	Si^{2+}	Si^{3+}	Si^{4+}
element (ADK calc)	0.24	0.95	7.8	14
HMDS (experiment)	0.56	0.77	1.5	3.0

[a] I_{sat} was determined by the method of Hankin et al.[21]

ionization rate. I_{sat} is defined as the point at which the ion yield (linear scale), extrapolated back from the high-intensity linear portion of the curve, intersects the intensity axis (logarithmic scale).[21] As no experimental data has been reported for pure silicon, the experimentally obtained I_{sat} of silicon for each charge state generated from HMDS was compared with I_{sat} of the element obtained by the Ammosov−Delone−Krainov (ADK) model based on a quasiclassical tunneling theory.[29] In the calculation of saturation intensity, a Gaussian (temporal and spatial) pulse was considered. Electron ejection from the *p* orbital (Si^{z+}, $z = 1-2$) and *s* orbital (Si^{z+}, $z = 3-4$) was assumed. We also assumed that the magnetic quantum number equals zero. Table 2 compares I_{sat} values. The ADK theory is known to overestimate the ionization rate in cases of singly charged metals[30] and molecules.[21] In other words, experimentally obtained I_{sat} is larger than that estimated by ADK theory, as was true for the singly charged silicon in our case. Comparing the I_{sat} in Table 2, triply and quadruply charged silicon was formed at a much lower laser intensity than that theoretically expected for the elements. The ease of highly charged ion production provides an important advantage when using organosilicon compounds as an ion source instead of pure silicon.

In broad terms, we now discuss and interpret the origins of the highly charged silicon ions. The vertical ionization energy of HMDS is 8.68 eV.[31] The ionization energies of silicon are 8.15 (Si), 16.3 (Si^+), 33.4 (Si^{2+}), and 45.1 eV (Si^{3+}), respectively.[32] Supposing that the highly charged silicon was produced from highly charged HMDS, the ionization potential of HMDS may be an important index. The ionization energy of $HMDS^+$ is unknown; however, we could estimate the ionization energy, as in the case of naphthalene.[33] We estimated the ionization energies of $HMDS^+$ and $HMDS^{2+}$ to be 15.2 and 22.7 eV, respectively. Although we cannot estimate the ionization energy of much higher charge states and hence I_{sat}, the enhancement of Si^{3+} and Si^{4+} production from HMDS compared with that predicted by the ADK theory for elements was presumably due to the increase in ionization energy of HMDS, as the charge state increase was much gentler than that for pure silicon due to the loose binding of electrons. It is evident that the fragmentation of $HMDS^{2+}$ and possibly of higher charge states immediately occurs because these ions are absent in the mass spectrum. Tunnel ionization would dominate any competitive processes above 10^{15} W cm^{-2}, and free silicon with a higher charge should be formed from the much higher charge states of HMDS.

Conclusion

The dissociation and multiply charged energetic atomic ion generation from HMDS was investigated by intense femtosecond laser pulses. Trimethylsilyl cation was the dominant fragment ion of HMDS as in the case of electron impact ionization. In addition, energetic trimethylsilyl cation was generated by the Coulomb explosion of doubly charged HMDS. Quadruply charged, neon-like silicon was formed in high abundance at high laser intensity. The threshold laser intensity of ion generation was compared with that obtained by quasiclassical tunneling theory. The production of triply and quadruply charged silicon from HMDS requires much less laser intensity than theoretically expected for isolated silicon. Due to the loose binding of electrons belonging to molecular orbitals, stripping electrons by tunneling from organosilicon compounds by laser electric fields is presumably much easier than from isolated silicon. Our results indicated that the femtosecond laser ionization of organosilicon compounds provides a great advantage in preparing highly charged energetic silicon, and hence has large potential for valuable applications.

Acknowledgment. The present research was partially supported by a Grant-in-aid from the Ministry of Education, Culture, Sports, Science and Technology, Japan, and by JST PRESTO program.

References and Notes

(1) Choy, K. L. *Prog. Mater. Sci.* **2003**, *48*, 57.
(2) Konuma, M., Ed. *Film Deposition by Plasma Techniques*; Springer-Verlag: Berlin, 1992.
(3) Hopwood, J. A., Ed. *Ionized Physical Vapor Deposition*, Academic Press: San Diego, 2000; Vol. 27.
(4) Wielunski, L. S.; Paterson, G. D.; Bell, J. M.; Clegg, R. E. *Nucl. Instrum. Meth. B* **2004**, *215*, 262.
(5) Currell, F. J., Ed. *The Physics of Multiply and Highly Charged Ions*; Kluwer Academic Pub.: Dordrecht, 2003; Vol. 1.
(6) Levis, R. J.; DeWitt, M. J. *J. Phys. Chem. A* **1999**, *103*, 6493. Nakashima, N.; Shimizu, S.; Yatsuhashi, T.; Sakabe, S.; Izawa, Y. *J. Photochem. Photobiol. C* **2000**, *1*, 131. Chin, S. L. In *Advances in Multiphoton Processsses and Spectroscopy*; Lin, S. H.; Villaeys, A. A.; Fujimura, Y., Eds.; World Scientific Pub. Co Inc: Singapore, 2005; Vol. 16, p 249.
(7) DeWitt, M. J.; Levis, R. J. *J. Chem. Phys.* **1995**, *102*, 8670.
(8) Ledingham, K. W. D.; Singhal, R. P.; Smith, D. J.; McCanny, T.; Graham, P.; Kilic, H. S.; Peng, W. X.; Wang, S. L.; Langley, A. J.; Taday, P. F.; Kosmidas, C. *J. Phys. Chem. A* **1998**, *102*, 3002.
(9) Chin, S. L.; Rolland, C.; Corkum, P. B.; Kelly, P. *Phys. Rev. Lett.* **1988**, *61*, 153.
(10) Yatsuhashi, T.; Nakashima, N. *J. Phys. Chem. A* **2008**, *112*, 5781. Yatsuhashi, T.; Nakashima, N. *J. Phys. Chem. C* **2009**, *113*, 11458.
(11) Tanaka, M.; Kawaji, M.; Yatsuhashi, T.; Nakashima, N. *J. Phys. Chem. A* **2009**, *111*, 12056.
(12) Campbell, E. E. B.; Hansen, K.; Hoffmann, K.; Korn, G.; Tchaplyguine, M.; Wittmann, M.; Hertel, I. V. *Phys. Rev. Lett.* **2000**, *84*, 2128. Tanaka, M.; Panja, S.; Murakami, M.; Yatsuhashi, T.; Nakashima, N. *Chem. Phys. Lett.* **2006**, *427*, 255.
(13) Murakami, M.; Tanaka, M.; Yatsuhashi, T.; Nakashima, N. *J. Chem. Phys.* **2007**, *126*, 104304.
(14) Harada, H.; Shimizu, S.; Yatsuhashi, T.; Sakabe, S.; Izawa, Y.; Nakashima, N. *Chem. Phys. Lett.* **2001**, *342*, 563. Harada, H.; Tanaka, M.; Murakami, M.; Shimizu, S.; Yatsuhashi, T.; Nakashima, N.; Sakabe, S.; Izawa, Y.; Tojo, S.; Majima, T. *J. Phys. Chem. A* **2003**, *107*, 6580. Murakami, M.; Mizoguchi, R.; Shimada, Y.; Yatsuhashi, T.; Nakashima, N. *Chem. Phys. Lett.* **2005**, *403*, 238.
(15) Bhardwaj, V. R.; Corkum, P. B.; Rayner, D. M. *Phys. Rev. Lett.* **2003**, *91*, 203004.
(16) Yatsuhashi, T.; Nakashima, N. *J. Phys. Chem. A* **2010**, *114*, 7445.
(17) Trushin, S. A.; Fuβ, W.; Schmid, W. E. *J. Phys. B* **2004**, *37*, 3987.
(18) Graham, P.; Ledingham, K. W. D.; Singhal, R. P.; Hankin, S. M.; Mccanny, T.; Fang, X.; Taday, P. F.; Langley, A. J.; Kosmidis, C. *Laser Part. Beams* **2001**, *19*, 187.
(19) Castillejo, M.; Martín, M.; de Nalda, R.; Couris, S.; Koudoumas, E. *J. Phys. Chem. A* **2002**, *106*, 2838.
(20) Castillejo, M.; Martín, M.; de Nalda, R.; Couris, S.; Koudoumas, E. *J. Phys. Chem. A* **2002**, *106*, 2838. Castillejo, M.; Martín, M.; de Nalda, R.; Couris, S.; Koudoumas, E. *Chem. Phys. Lett.* **2002**, *353*, 295.
(21) Hankin, S. M.; Villeneuve, D. M.; Corkum, P. B.; Rayner, D. M. *Phys. Rev. A* **2001**, *64*, 013405.
(22) Takeuchi, T.; Tanaka, M.; Matsunani, T.; Kiuchi, M. *Surf. Coat. Technol.* **2002**, *158*, 408.
(23) Yatsuhashi, T.; Murakami, M.; Nakashima, N. *J. Chem. Phys.* **2007**, *126*, 194316.
(24) Cornaggia, C.; Lavancier, J.; Normand, D.; Morellec, J.; Agostini, P. *Phys. Rev. A* **1991**, *44*, 4499.
(25) Imamura, T.; Ce, B.; Koyano, I.; Ibuki, T.; Masuoka, T. *J. Chem. Phys.* **1991**, *94*, 4936.

(26) Shimizu, S.; Zhakhovskii, V.; Sato, F.; Okihara, S.; Sakabe, S.; Nishihara, K.; Izawa, Y.; Yatsuhashi, T.; Nakashima, N. *J. Chem. Phys.* **2002**, *117*, 3180.

(27) Yatsuhashi, T.; Obayashi, T.; Tanaka, M.; Murakami, M.; Nakashima, N. *J. Phys. Chem. A* **2006**, *110*, 7763.

(28) Bescós, B.; Hoch, R.; Schmidtke, H.-J.; Gerber, G. *Appl. Phys. B: Laser Opt.* **2000**, *71*, 373.

(29) Ammosov, M. V.; Delone, N. B.; Krainov, V. P. *Sov. Phys. JETP* **1986**, *641*, 1191.

(30) Smits, M.; de Lange, C. A.; Stolow, A.; Rayner, D. M. *Phys. Rev. Lett.* **2004**, *93*, 213003.

(31) Mochida, K.; Worley, S. D.; Kochi, J. K. *Bull. Chem. Soc. Jpn.* **1985**, *58*, 3389.

(32) Cowan, R. D. *The Theory of Atomic Structure and Spectra*; University of California Press: Berkeley LA, 1981.

(33) Yatsuhashi, T.; Nakashima, N. *J. Phys. Chem. A* **2005**, *109*, 9414.

JP1067186